# Supplementary Information

## Multi-channel information encryption based on the structural color and photoluminescence capability of cellulose nanocrystals flexible films

Xu Li [a, b], Yuzhou Chen [a, b], Yunlong Dong [a, b], Yang Li [a, b], Yuelan Lv [c*], and Yongjun Liu [a, b *]

[a:] Key Laboratory of Photonic Materials and Devices Physics for Oceanic Applications, Ministry of Industry and Information Technology of China, College of Physics and Optoelectronic Engineering, Harbin Engineering University, Harbin 150001, China

[b:] Key Laboratory of In-Fiber Integrated Optics of Ministry of Education, College of Physics and Optoelectronic Engineering, Harbin Engineering University, Harbin 150001, China

[c:] College of Mechanical and Electrical Engineering, Guangdong University of Science and Technology, Dongguan, 523083, China

*Corresponding authors：Yongjun Liu liuyj@hrbeu.edu.cn;

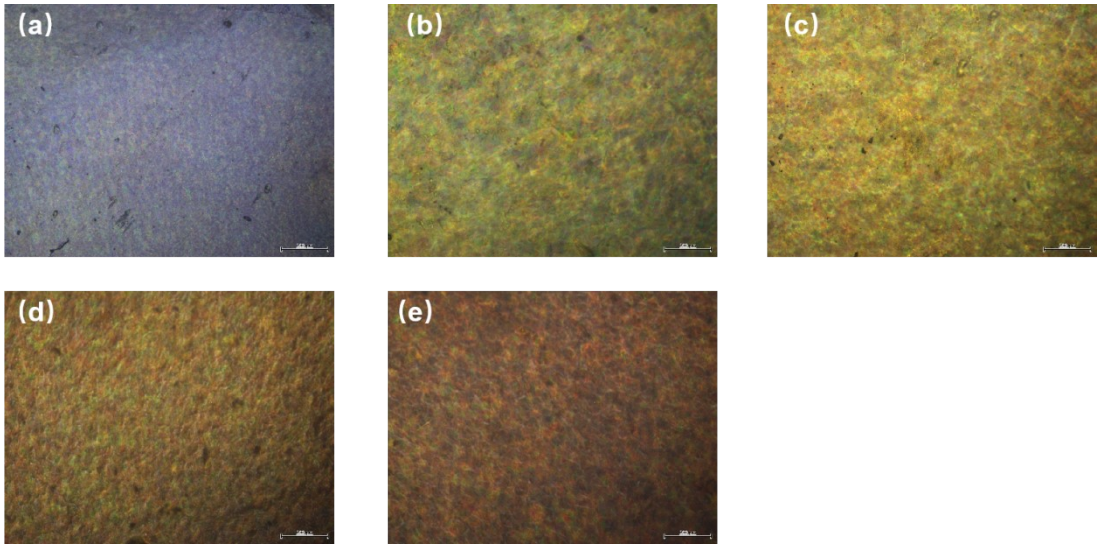


**Figure S1.** a) Photographs of CGP10, b) CGP15, c) CGP20, d) CGP25, and e) CGP30 composite films under a reflectance microscope (scale bar: 200 μm).

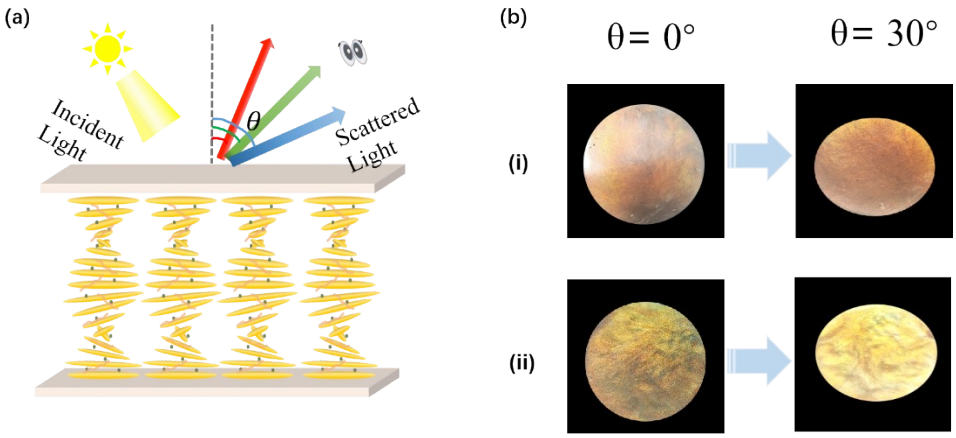


**Figure S2.** a) Schematic illustration of the angular dependence of the chiral nematic structure; b) Photographs of (i) CGP30 and (ii) CGP25 composite films at viewing angles of 0° and 30°, respectively.

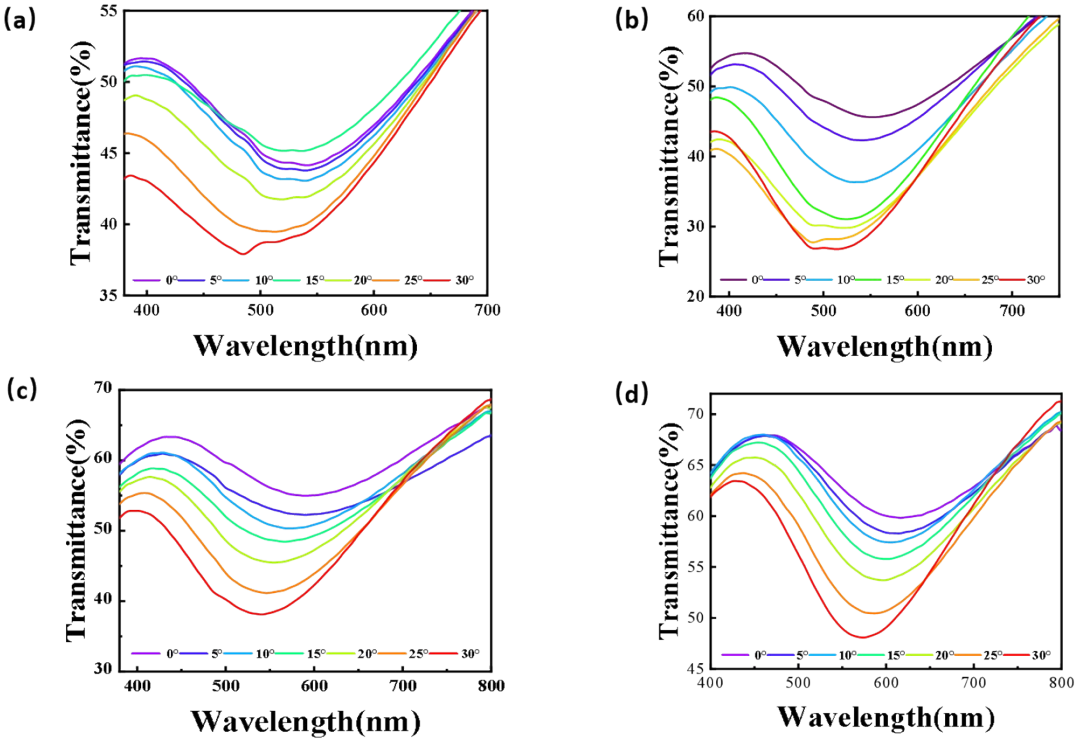


**Figure S3.** Transmission spectra corresponding to a) CGP10, b) CGP15, c) CGP20, and d) CGP25 composite films with viewing angle from 0° to 30°, respectively.

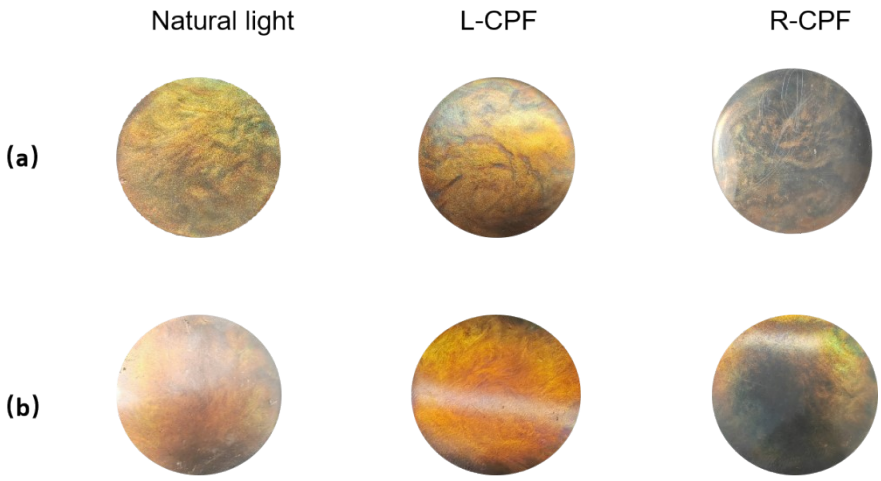


**Figure S4.** Photographs corresponding to a) CGP25, b) CGP30 composite films under natural light, left circularly polarized light, and right circularly polarized light, respectively.

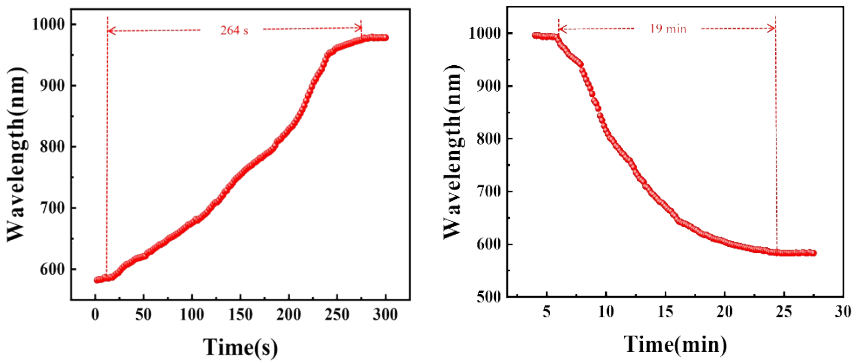


**Figure S5.** CGP20 film humidity (a) response time (b) recovery time

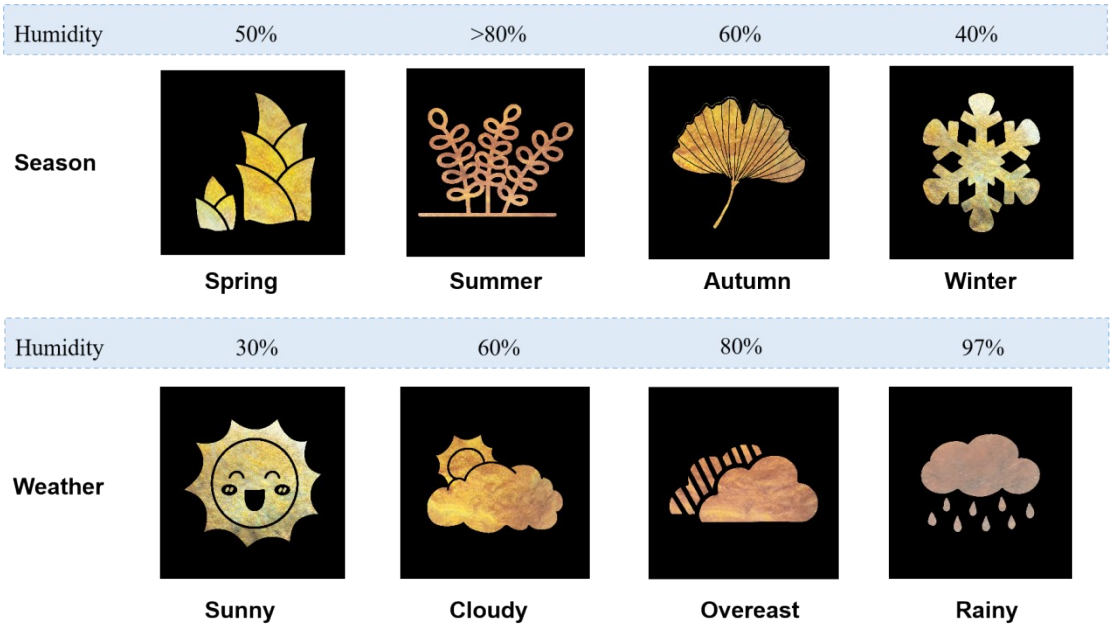


**Figure S6.** Structured color films in smart displays, structured color changes of photonic patterns under spring, summer, autumn and winter seasons, structured color changes of photonic patterns under different weather conditions (sunny, cloudy, cloudy, rainy).

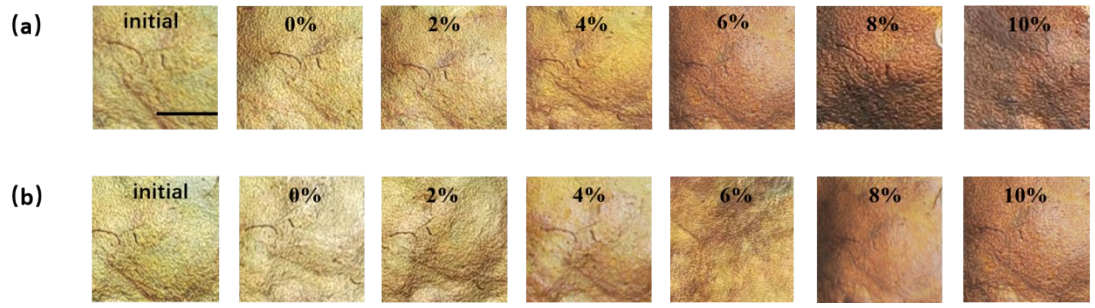


**Figure S7.** Photographs of color changes of CGP20 films immersed in solutions with different water contents of a) ethanol and b) THF (Scale bar:5 mm).

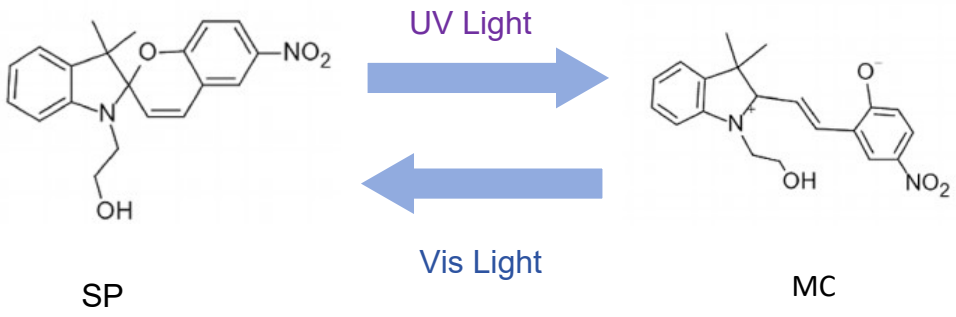


**Figure S8.** Structural formulae for the reversible isomerization of spiropyrans between closed-loop (SP) and open-loop (MC) structures.

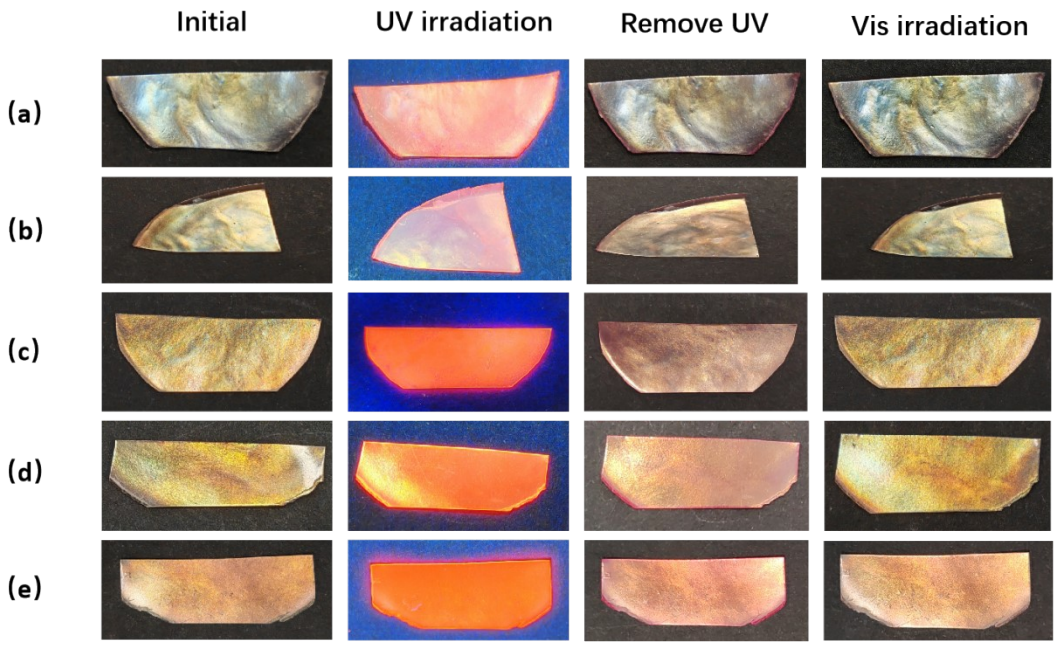


**Figure S9.** Photographs of cut sections a) SP-CGP10, b) SP-CGP15, c) SP-CGP20, d) SP-CGP25, and e) SP-CGP30 composite films in the initial state, during UV irradiation, after removal of UV lamps, and during white light irradiation.

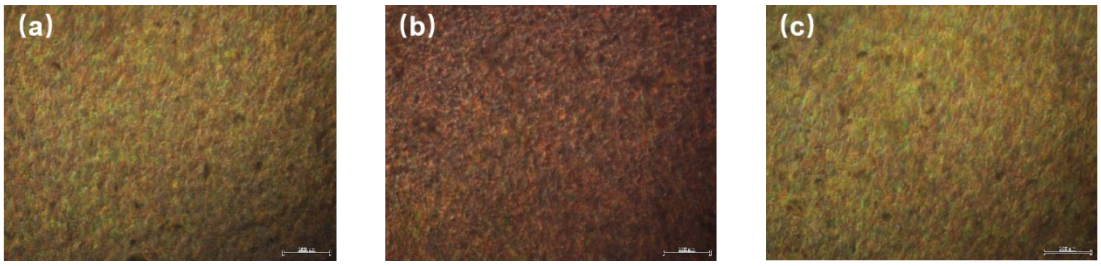


**Figure S10.** Pictures of SP-CGP25 composite films under a reflectance microscope in (a) the initial state, (b) after irradiation by UV light, and (c) after irradiation by white light (scale bar: 200 μm).

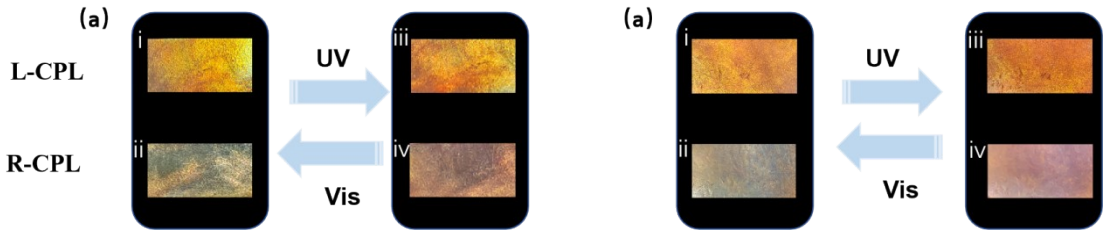


**Figure S11.** Photographs of a) SP-CGP25 composite film and b) SP-CGP30 composite film under left-rotating circular polarizer and right-rotating circular polarizer after irradiation by visible light (i)(ii) and UV light (iii)(iv), respectively.

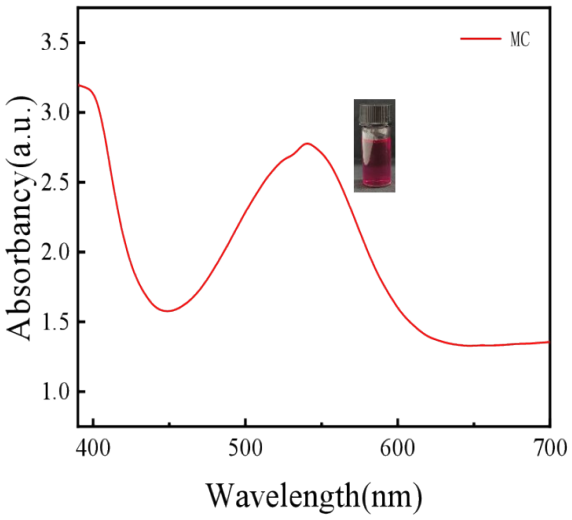


**Figure S12.** Absorption spectra of spiropyran solutions in the ring-opened MC state after UV irradiation.

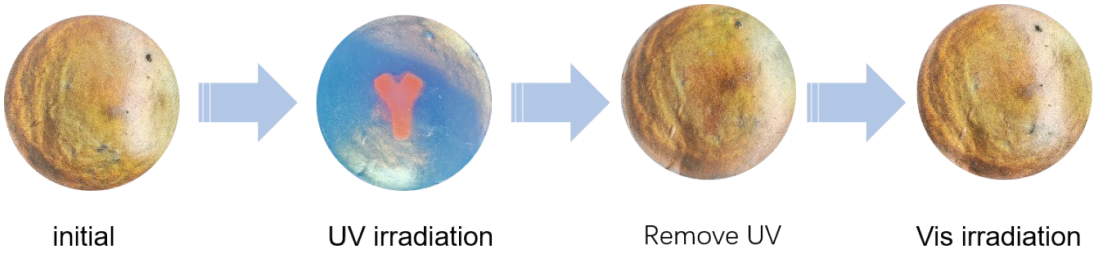


**Figure S13.** Simple letter "Y" encryption realized by combining the chiral photonic properties of the CNC host matrix with the photochromic coloration of the SP.

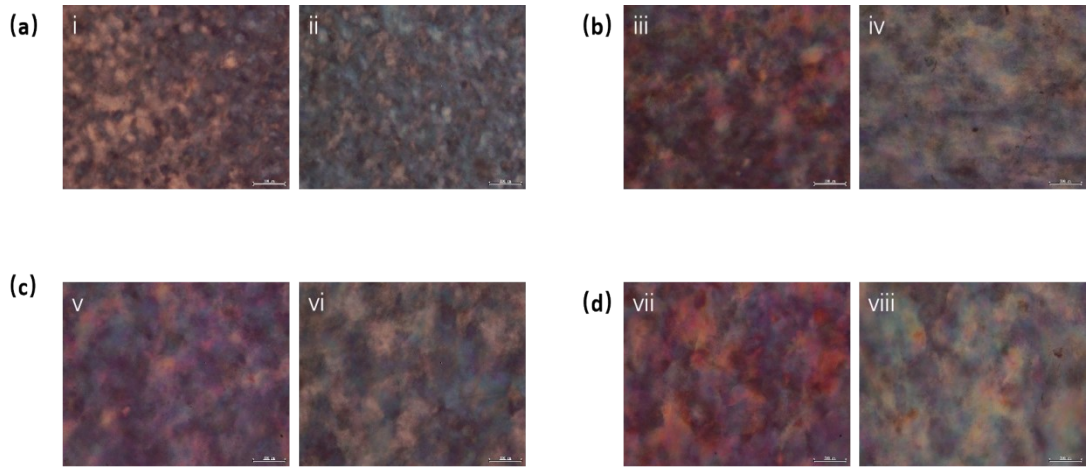


**Figure S14.** a) POM images of SP-CGP10, b) SP-CGP15, c) SP-CGP20, and d) SP-CGP25 composite films after UV irradiation (i)(iii)(v)(vii) and after white light irradiation (ii)(iv)(vi)(viii) (scale bar: 100μm).